The Abdus Salam
International Centre for Theoretical Physics

EMAS 2008

8th EMAS Regional Workshop on

Electron Probe Microanalysis of Materials Today

Practical Aspects

including a session on

synchrotron-based microanalysis

19 - 22 April 2008

Adriatico Guesthouse
The Abdus Salam International Centre for Theoretical Physics
Trieste, Italy

Book of Abstracts

SAMPLE PREPARATION FOR EPMA

Silvia Richter* and J. Mayer

R.W.T.H. Aachen, Central Facility for Electron Microscopy (GfE)
Ahornstrasse 55, DE 52074 Aachen, Germany
** richter@gfe.rwth-aachen.de*

INTRODUCTION

What are the demands on preparation which we have to consider for measuring the true chemical structure of a sample? First of all, the material's composition should remain unchanged within the excitation volume. Furthermore, since the measured X-ray intensities have to be converted into elemental concentrations or mass coverages with the help of quantification procedures, the assumptions used in these procedures have to be fulfilled. Typically, the models assume conductive samples with flat surface and with a defined tilt angle towards the electron beam. Each deviation from these conditions, like surface roughness or charging effects, can lead to an erroneous analysis of the chemical structure. Thus, sample preparation is an important issue in EPMA.

Since most of the preparation techniques for light microscopy can be used, the associated research fields, like metallography or nowadays called materialography, deliver a wide range of preparation recipes. Therefore, it is not the aim of this article to give an all-inclusive recipe, but to impart knowledge about the basic steps and possible artefacts.

SAMPLING

In many cases materials received by the laboratory are usually larger than that required for the measurement. Thus, preparation starts with the question: Which size and how many samples do I need for the measurement? The maximum size of the sample analysed depends on the design of the sample holder of the chosen instrument. For example, the microprobe at our laboratory has the following types of holders (Fig. 1).

The maximum size of the sample is 1 or 1½ inch in diameter and 20 mm in height, including mounting material or wall thickness of the holder.

A given heterogeneity of the original material results in the selection of many samples representative of a special property or treatment of the material. A properly designed sampling plan has then to be written. The number of samples can be estimated by statistical methods [1, 2] or often it is a compromise between heterogeneity and costs. When the properties of the material are unknown, the best way is to start with a small number of samples, using

Fig. 1. EPMA sample holders available at the GFE.

experience and intuition as a guide to make them as representative of the received material as possible, and to perform the corresponding measurements. In an iterative way one then has to evaluate the results and to decide on the further procedure.

SECTIONING

Many different methods [3, 4] can be used for sectioning materials, i.e. cleaving, fracturing, sawing, cutting and wire EDM. In all cases, the near-surface region of the sectioned surface is damaged more or less deeply. The depth of damage varies with material and sectioning method. Subsequent operations like grinding and polishing have to be performed in order to remove the damaged material. The focus of this article will be a short description of two commonly used methods, i.e. abrasive cutting and wire sawing. Finally, an incorrect preparation technique is reported, where a laser was used for cutting.

Abrasive cutting

Many types of abrasive wheels are offered by different manufacturers. The type is determined by the sort of abrasive grains, their bonding, and the porosity of the wheels. As a rule of thumb, hard bond wheels cut soft materials and soft bond wheels cut hard materials. In order to minimise the depth of damage during sectioning it is recommended to follow the instructions of the manufacturers concerning the choice of abrasive wheel, lubricant/ coolant and operating conditions.

For precision cutting and for cutting extremely hard materials, diamond-impregnated wheels are preferred. Such low speed diamond saws (Fig. 2) cut slowly, but the as-cut surface is relatively smooth and further preparation time is short. Additionally, the possibility of dry-cutting prevents contamination from the lubricant.

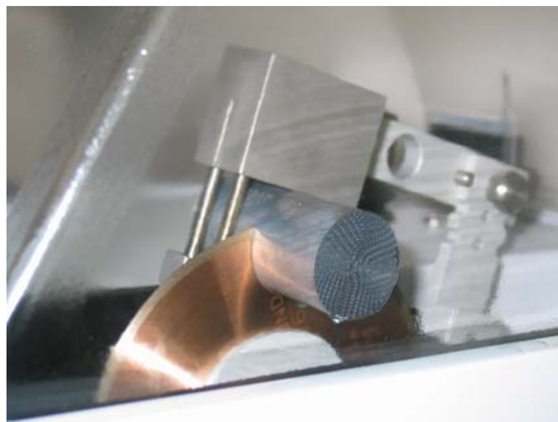

Fig. 2. Low-speed diamond saw.

Wire saw

The device with highest precision, lowest damage and lowest contamination is the wire-saw (Fig. 3). In principle, a fine diamond-impregnated wire is the cutting tool. Although cutting rates are much lower than those of abrasive wheels the damage produced is negligible and subsequent grinding and polishing is often not necessary. It is a nearly contamination-free sizing method, since water is not used as lubricant, but it is only used to wash out the debris that would accumulate above the wire.

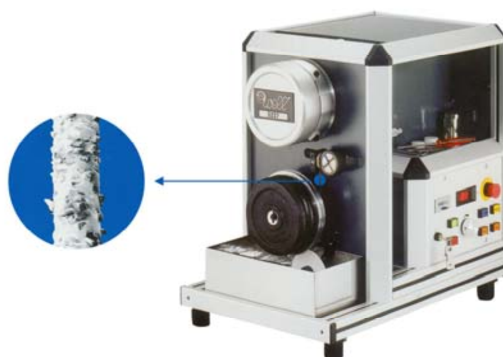

Fig. 3. Wire-saw.

Laser induced cutting

This can be applied to a metal sheet of which an oxide scale and/or corrosion products have to be examined by EPMA. In order to avoid contamination of the surface and to have a rapid method for preparing a lot of samples, pieces of 1 cm × 1.5 cm were cut from the sheet

metal by a laser process (Fig. 4). Deposition of removed material during the process was prevented by a steady gas flow.

Fig. 4. Laser induced cutting.

Since the focus of the laser beam was not well adjusted, the laser induced heat produces a damaged zone down to a depth of about 100 µm (see Fig. 5). The damage was not sufficiently removed in the subsequent cross-section preparation steps. As a result, the oxide scale was erroneously analysed as combined corundum $(Cr,Al)_2O_3$ (Fig. 6). Yet, the true oxide scale (Fig. 7), which consists of an outermost Cr_2O_3-layer with an oxidation of Al at the grain boundaries, was finally uncovered after further steps of grinding and polishing. Knowledge about the depth of damage or correspondingly, knowing how much material has to be removed, is an important issue for EPMA. Incorrect preparation techniques may alter the true microstructure and lead to erroneous conclusions.

Fig. 5. Laser-induced heat damage zone.

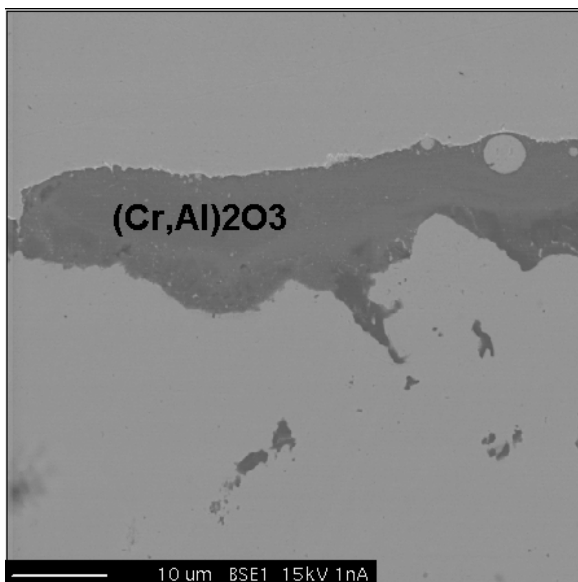

Fig. 6.

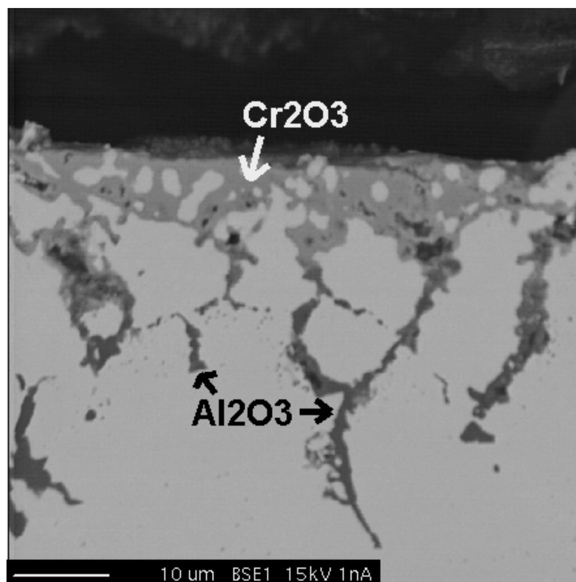

Fig. 7.

FIXING AND MOUNTING

For quantitative X-ray analysis the specimen's surface has to be flat and perpendicular to the electron beam. Alternatively, if in-situ tilting is possible, the tilt angle has to be determinable for a correct matrix correction. Mounting the specimen is essential both (i) for save handling of small and oddly shaped specimens during grinding and polishing, and (ii) for inserting the specimens in the electron microscope in an acceptable geometric way (under well-defined geometric conditions). The geometry of the mounts depends on the design of the sample holder. For simplicity's sake, this design is adapted to the one for metallographic examinations. Alternatively, an unmounted specimen can be embedded into an Al-foil under the pressure of a dye (Fig. 8). For the analysis of a thin film a piece of coated wafer can be fixed on a face of a holder by using an adhesive tape or silver paint (Fig. 9).

Fig. 8.

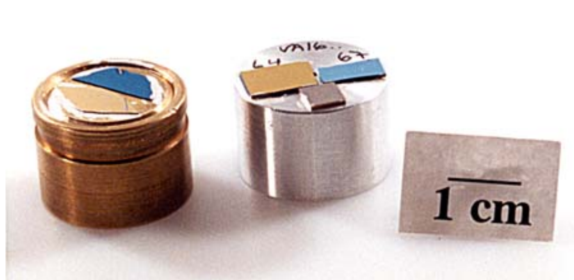

Fig. 9.

Which embedding material?

First of all, the mounting material must be vacuum-compatible. Then the basic metallographic requirements have to be fulfilled. The abrasive removal characteristics of mounting material and specimen must be similar in order to get an overall flat surface. The shrinkage of the resin must be small. A gap between specimen and resin can include rests of polishing material, which outgases in an electron microscope producing a bad vacuum and contaminates the edges (see Fig. 10). For EPMA an electrically conductive resin is desirable, especially for long-term measurements.

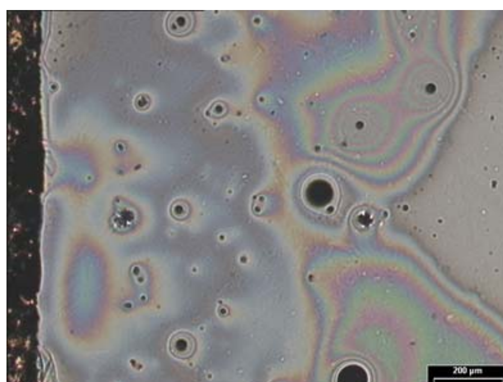

Fig. 10.

Two main classes of mounting materials are commercially available:

Compression-mounting materials (or hot-mounting materials)

If the material is resistant to heat up to about 180 °C and to a pressure up to about 30 Mpa, compression-mounting is preferable due to the high vacuum compatibility. Diallyl phtalate provides relatively hard mounts and good edge retention. With the addition of a conductive filler, like copper, it is an excellent mount for electron microscopy (Fig. 11). Sometimes, the conductivity of this type of mounting fails. This can be caused by a too big size of copper particles, or by oxidation of the copper. The use of fresh mounting powder or pounding of the powder before mounting is then recommended. Alternatively, phenolic as a resin filled with carbon can be used.

Cold-mounting materials

Epoxies as resins are acceptable for vacuum conditions, though curing time depending on formulation vary from 1 to about 8 hours. Be careful with other quick-curing resins, the strong emission of gases could be a problem for the microscope (contamination of apertures) and of course for the analysis. Due to the good adherence and low viscosity, epoxies are used for vacuum-impregnation of porous or brittle specimens. Vacuum-impregnation promotes the filling of voids, prevents contamination and also prevents loss of loose components. Nevertheless, epoxies produce a small amount of vapour contamination. Grinding down the

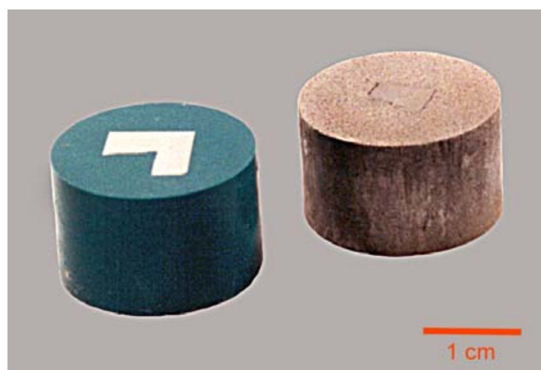

Fig. 11.

material of 1 - 2 mm in height at the bottom of the mounted specimen could improve the vacuum compatibility, because sometimes the hardener is evaporated during mounting. Overnight storage in a low temperature oven or longer pre-pumping in a coating device results in the removal of the remaining volatile components. Epoxy is not very stable under electron beam exposure. Measurements have to be performed with minimum beam time on the mounting material. For vacuum-impregnation the use of conductive fillers could be a challenge, since the fillers increase the viscosity of the epoxy, preventing a poreless mounting material.

PLATING

Specimens for which it is necessary to examine the edges or the near-surface region (e.g. oxide scales or corrosion zones) are often plated before mounting, to prevent edge rounding. A relatively unproblematic and proven method is electrolytically plating with Ni. The precondition is a conductive coating like gold, which can be sputtered on the specimen's surface. Afterwards, the specimen is put into a Ni-bath solution (see Table 1) as the cathode. By connecting a Ni-sheet to the positive pole and using a stirrer for bath motion, a Ni-layer of about 60 µm thickness is deposited after 6 hours at a current density of about 25 mA/cm². Fig. 12 shows a cross-section of a high temperature steel, where the corrosion zone is the region of interest. Surrounded by the Ni-layer, the flat and crack-free region is an ideal condition for EPMA, especially for light element analysis.

Table 1. Composition of the Ni-plating solution.

30 g $H_4N_2NiO_6S \times 4H_2O$ (nickel(II)sulphamate)
31 g $NiCl_2 \times 6H_2O$ (nickel(II)chloride hexahydrate)
31 g H_3BO_3 (boric acid)
1 l distilled H_2O

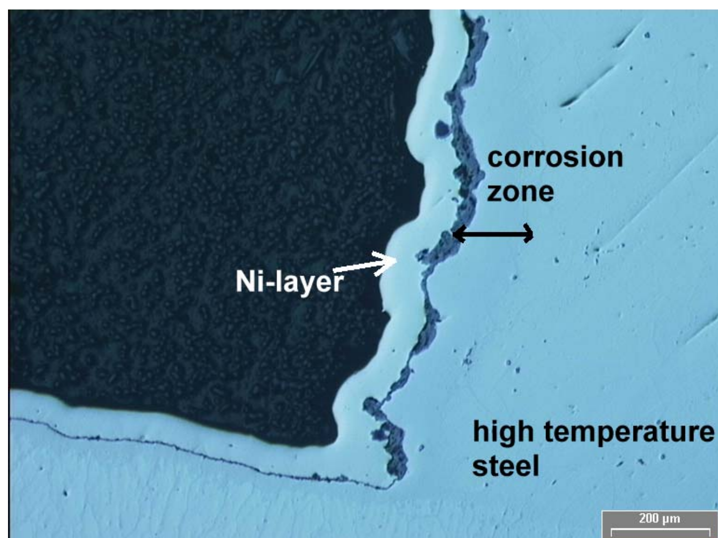

Fig. 12. Cross-section of a high-temperature steel.

GRINDING AND POLISHING

EPMA should be performed on flat specimens. The erroneous analysis of specimens with rough surfaces can be demonstrated by tilting the specimen relative to the direction of the electron beam towards (positive tilt angle) and straight off the detector (negative tilt angle) for simplicity's sake. For a material consisting mainly of Fe, the relative X-ray intensities of B-Kα, C-Kα, Al-Kα and Ti-Kα plotted versus tilt angle, are shown in Fig. 13. The incident electron beam energy is 7 kV and the detector's take off angle is 40°. The calculation is based on a Monte-Carlo simulation [5].

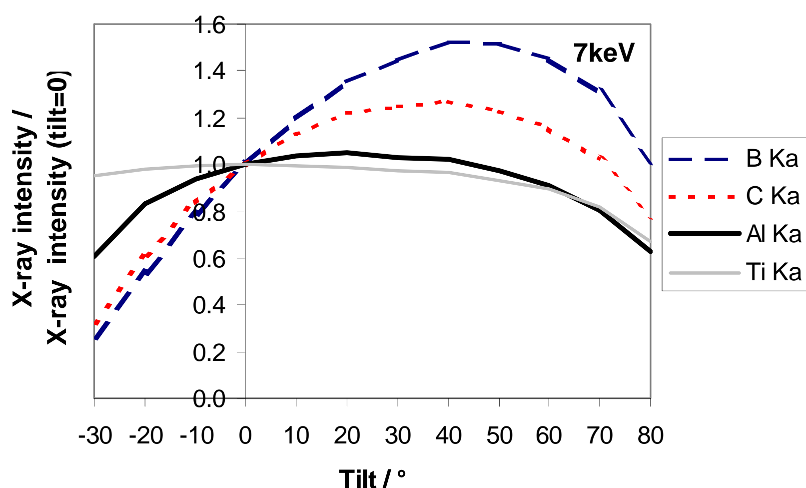

Fig. 13. Plot of the relative X-ray intensities of B-Kα, C-Kα, Al-Kα and Ti-Kα versus tilt angle.

In particular, for light element analysis, where high mass absorption coefficients and low information depths are expected, the relative error can amount to about 50%. Further details about quantitative X-ray microanalysis and roughness are described by Gauvin et al. [6]. Therefore, grinding and polishing is an unavoidable procedure in specimen preparation for EPMA. Well-established [3, 7, 8] metallographic preparation procedures can be employed, i.e. a sequence of grinding stages of increasing fineness, followed by a sequence of polishing processes of increasing fineness until the desired surface finish has been achieved. It is well known that grinding produces scratches and imposes severe plastic deformations on the outer layers of the surface. Polishing procedures are similar, except that only small forces are applied to individual abrasive particles by the fibres of the cloth that supports them. They therefore produce shallow, narrow scratches. The diagram in Fig. 14 illustrates the thickness of the resulting fragmented layer, dominated by scratches, and of the deformation layer lying underneath [9]. The damaged region including deformation is also of importance in the quantitative X-ray microanalysis of non-conductive specimens, where charging is a severe problem [10]. A disordered material's structure offers more trapping sites for incidents electrons than a perfectly ordered one. This effect was proven by Remond et al. [11]. Finally, with increasing fineness of the abrasives the heat transfer to the specimen surface will be negligible and therefore only an oxide layer with a thickness of a few nm can be expected for metals.

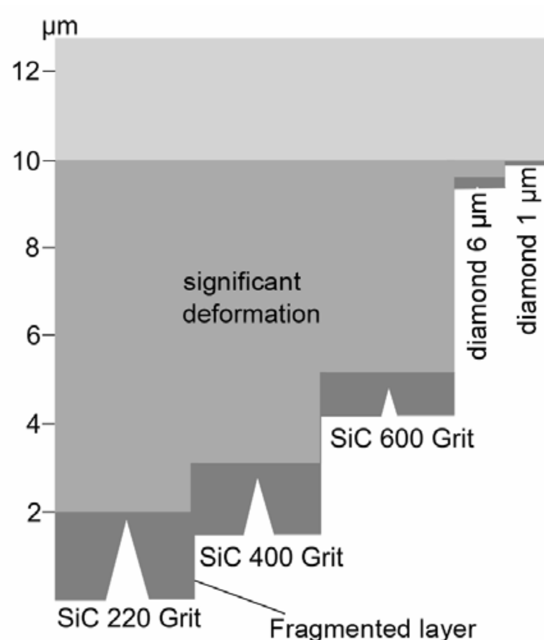

Fig. 14. Thickness of the fragmented layer produced by polishing, dominated by scratches, and of the deformation layer lying underneath.

For grinding, waterproof abrasive papers, usually those coated with silicon carbide abrasive, are convenient. Due to their low cost, SiC-papers can be freshly used for each preparation to avoid contamination from preceding ones. Diamond, alumina and colloidal silica are the most commonly used abrasives for polishing. Colloidal silica has to be avoided when analysing oxygen, since a thin amorphous glass film may be deposited on the surface. Soft materials can smear during polishing and contaminate their surrounding surface area. Because of this smearing the chemical analysis, especially the determination of the copper concentration, could fail using the copper filled mounting material. Furthermore, fragments of abrasives may become embedded in the surface of metal samples. Thus, thoroughly cleaning after each preparation stage is necessary. After the last one, an ultrasonic bath in ethanol is recommended for removing rests of lubricants and polishing suspensions in pores, cracks and crevices. In trace analysis or analysis at edges, a careless cleaning could lead to a misinterpretation of the specimen's chemistry.

PLASMA CLEANING

The application of plasma cleaning is an excellent method for eliminating hydrocarbon contamination from the specimen. During a measurement there are two main causes of contamination build-up at the impact point of the electron beam. The first source of contamination is the migration of existing surface contamination to the electron beam.

Surface contamination may result from specimen preparation due to inadequately removed solvents or chemicals. It can be extremely difficult to prepare a perfectly clean sample. The other source of contamination is due to hydrocarbons originating from the vacuum system of the SEM or microprobe. The emission of gases from mounting material and the oil of the diffusion pumps can influence the vacuum conditions. Hydrocarbons are cracked by the incident electrons, and carbon, one of the reaction products, is deposited on the specimen's surface around the impact point. Fig. 15 shows a typical contamination structure caused by this process.

As can be imagined, severe problems may exist in light-element analysis, especially the analysis of carbon, and in low-voltage applications. For example, without any anti-contamination devices, a carbon content of about 0.5% is measured in an IF-steel ($C < 0.01\%$) using an electron microprobe Camebax SX 50 with the following conditions: electron beam energy: 15 keV, beam current: 100 nA. Thus, the determination of carbon concentrations lower than 1% is a challenge and one step on a successful way is plasma cleaning [11]. Plasma cleaning [12] relies on the application of a high-frequency, low-energy reactive gas plasma. Various process gases may be used during plasma cleaning to sputter or, more effectively, to induce chemical reactions with the hydrocarbon contamination. The most effective gases for eliminating hydrocarbons are oxygen and hydrogen. Dissociated oxygen atoms created by the plasma chemically react with hydrocarbons by converting them to volatile products like CO, CO_2 and H_2O. The effectiveness of this preparation process is shown in Fig. 16 by measuring the contamination rate, i.e. the C-Kα intensity versus time of electron beam exposure, on a steel

surface for different anti-contamination devices. The lowest contamination rate is achieved using an additional plasma cleaning process.

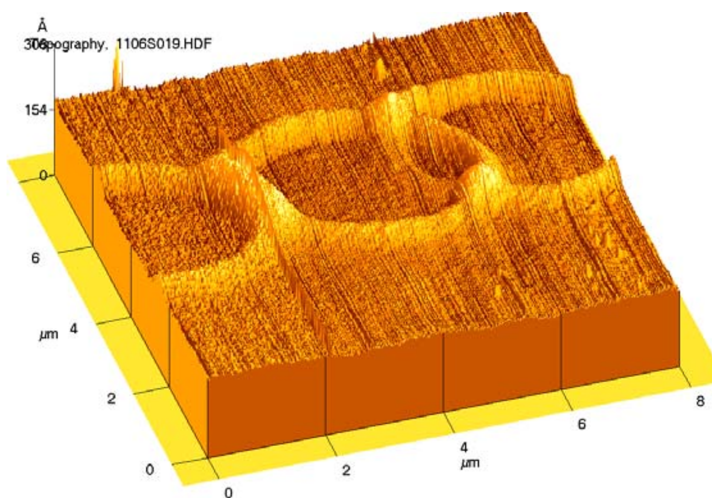

Fig. 15. Typical contamination structure caused by cracking of hydrocarbons by the incident electrons.

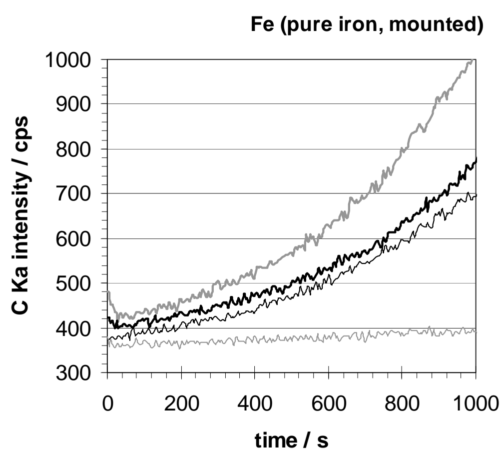

Fig. 16. Measurement of the contamination rate, i.e. the C-Kα intensity versus time of electron beam exposure, on a steel surface for different anti-contamination devices.

CONDUCTIVE COATING

The final step before the sample is inserted into the SEM or the microprobe may be to coat the sample with a thin conductive layer [13]. This is unavoidable for non-conductive specimens, but sometimes it is also recommended for porous conductive specimens embedded

in a non-conductive mounting material. Carbon or metal films like gold are widely used for coating.

Gold is used most often for contrast enhancement in imaging by using the shadowing effect. When performing X-ray analysis, the primary and back-scattered electrons from the specimen can excite X-ray radiation in the coating that can interfere with the X-ray lines of interest, e.g. gold with zirconium, phosphorus, or platinum. Therefore, the preferred coating element for X-ray analysis is carbon, because it has a minimal effect on the X-ray spectrum.

Another argument is the low mass absorption coefficient of many X-ray lines in carbon. Exceptions are the analysis of light elements. Copper coating is often used in the case of O-Kα due to the lower absorption coefficient in comparison to carbon, but Bastin et.al. [14] demonstrate an erroneous quantitative analysis due to a remaining charging effect in the underlying non-conductive specimen. They recommend performing measurements at higher voltages or through a hole in a carbon coating. The hole can be burned in a carbon coating by using an air jet.

Edge rounding

If the region between two phases of different hardness is of interest for X-ray microanalysis, edge rounding has to be avoided during preparation. In the following example, the aim was to study the reaction zone between corundum grains and its surrounding matrix consisting of glass. Since corundum is a very hard material, the specimen was grinded on a diamond disc. Diamond lapping is known for producing an excellent flat surface at the transition corundum-glass. Furthermore, for optimum flatness use of an automatic device, the Buehler Minimet, is preferred to manual operation, because the applied pressure is more even. Finally, the specimen was shortly polished on a perforated short-nap cloth. Fig. 17 shows the light-microscopic image of the prepared specimen surface. Chipping artefacts are still visible due to the short polishing time. Very hard materials, like corundum, are inherently brittle and tend to develop chipping artefacts. Be careful not to misinterpret them as pores. In our case, a short polishing time was preferred to minimise edge rounding. Nevertheless, the perfect flatness was not achieved. The backscattered electron image (Fig. 18) makes the residual roughness stand out by using the topographic mode. The height of the edge is about 100 nm, as determined by AFM (Fig. 19). This small roughness was sufficient to cause errors in X-ray microanalysis. In particular, the analysis of light elements, like oxygen, was a problem. Measuring the O-Kα intensity (Fig. 20) along a line across the region corundum-glass–corundum revealed that strong intensity variations occurred at both phase boundaries. These artefacts are caused predominantly by absorption effects and can be explained as follows: The edge pointing away from the detector is shadowing the emitted O-Kα intensity due to a longer absorption path, whereas the opposite edge (directed towards the detector) delivers a higher intensity due to a shorter absorption path. As a result, materials containing phases of different hardness are often a challenge for a mechanical preparation. A possible solution could be the use of ion beam techniques in sample preparation.

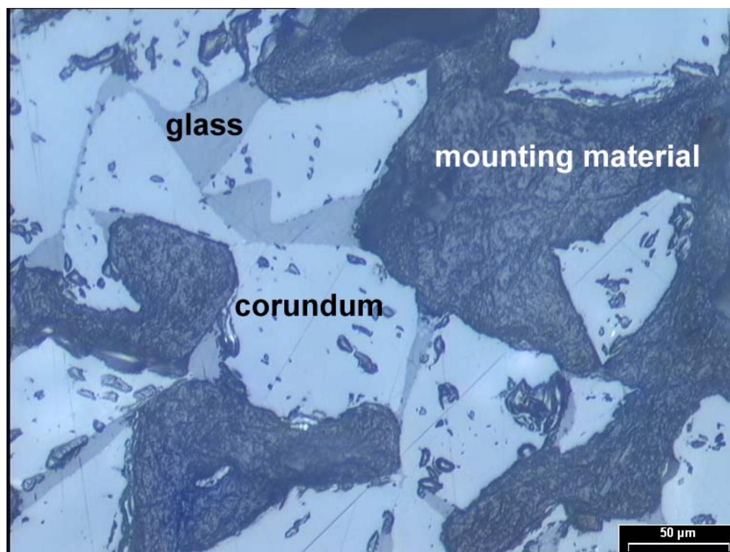

Fig. 17. Light-microscopic image of the prepared specimen surface.

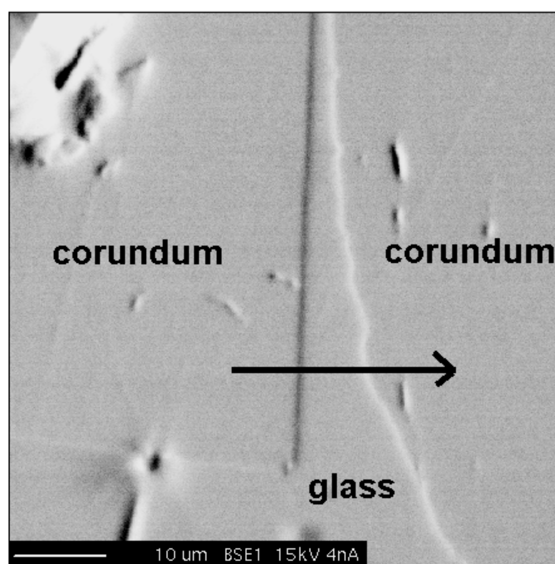

Fig. 18. Backscattered electron image, using the topographic mode, showing the residual roughness.

ELECTROLYTIC POLISHING

Electrolytic polishing [15] is widely used in the preparation of metals or metal alloys which are difficult to polish by mechanical methods. It is preceded by mechanical grinding. A typical setup is shown in Fig. 21. The cathode and the specimen (anode) are suspended in a container filled with the electrolyte. By applying a voltage, a reaction starts between the

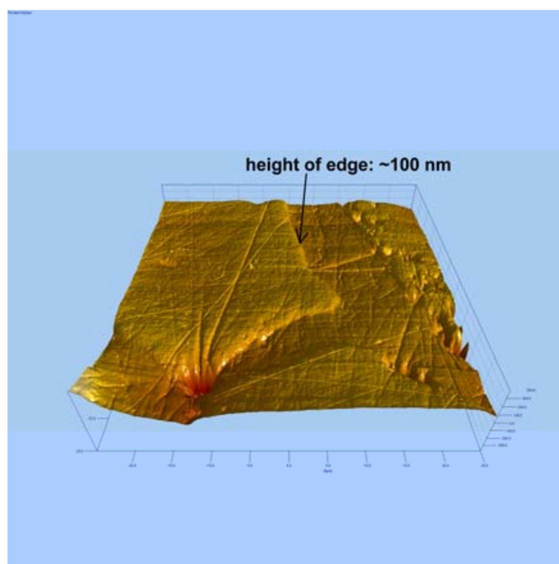

Fig. 19. AFM determination of the height of the edge, estimated to be about 100 nm.

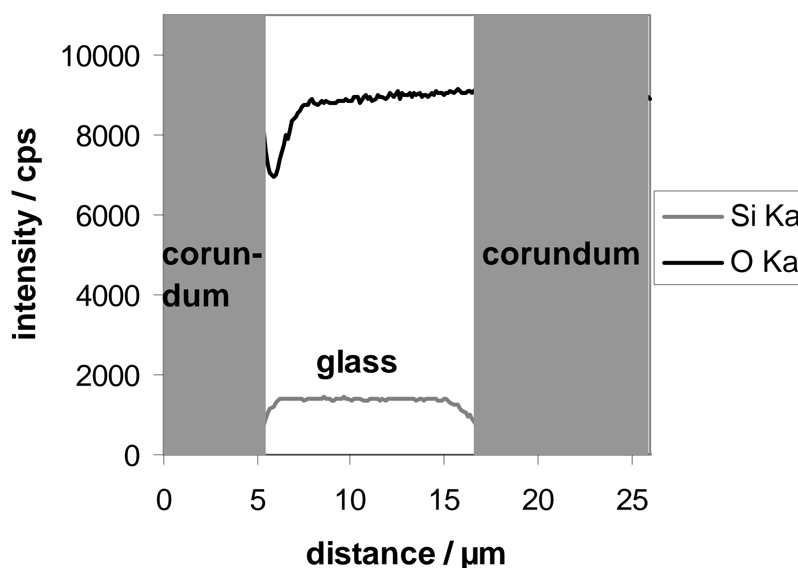

Fig. 20. Measurement of the O-Kα intensity along a line across the region corundum-glass–corundum interfaces.

specimen surface and the electrolyte. The quality of the polishing depends on the current-voltage relationship, which varies for different electrolytes and metals.

Smoothing is accomplished because higher points of the surface experience higher currents. Thus, at these spots material is dissolved faster than in the surrounding areas, leading to a gently undulating surface. The morphology of an electro-polished surface of an Al alloy is

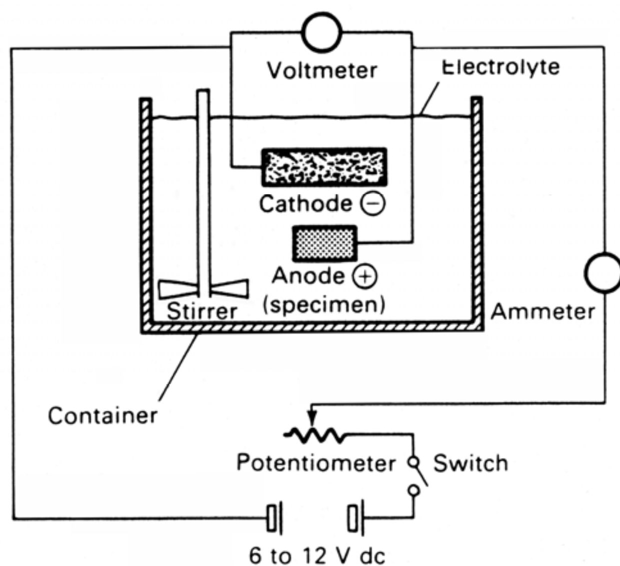

Fig. 21. Typical electro-polishing setup.

presented in Fig. 22. For comparison, the morphology of the mechanically prepared surface is also shown (Fig. 23). The recipes of both methods are listed in Table 2. Indeed, the electro-polished surface may be slightly undulated, in contrast to the perfectly flat one of the mechanically polished surface. Scratches occur only in the latter. The mean roughness of the mechanically polished surface is about 10 nm, whereas a value of 100 nm is achieved for the electro-polished surface. However, for quantitative X-ray analysis the local tilt angles have to be considered. Therefore, maximum tilt angles of ±1.5° are evaluated from the height profile of the electro-polished surface (Fig. 24). As a result, quantitative X-ray analysis can be performed on electro-polished surfaces, if the desired sensitivity is sufficient or limited by other errors like statistic ones.

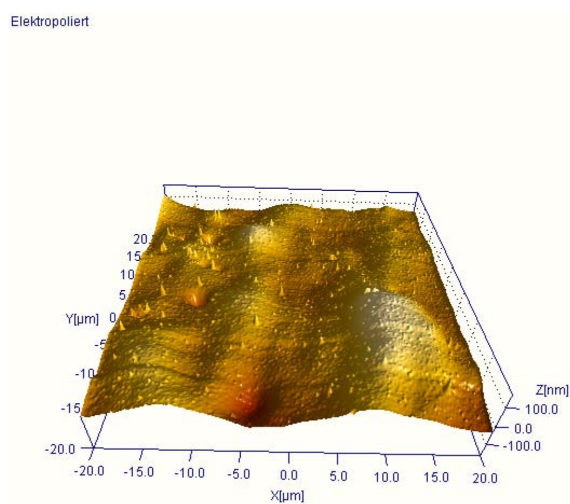

Fig. 22. Morphology of an electro-polished surface of an Al alloy.

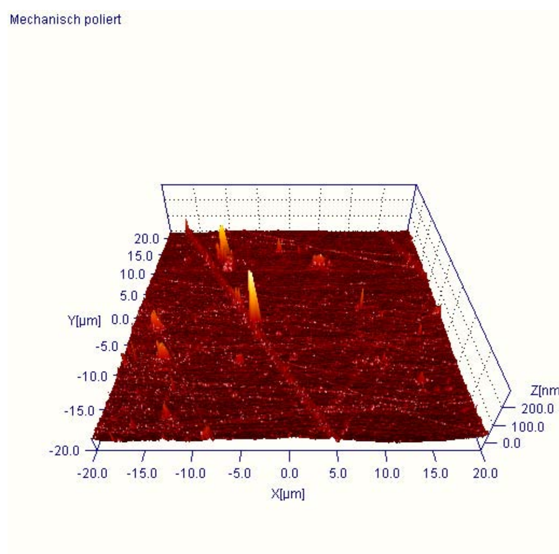

Fig. 23. Morphology of a mechanically prepared surface of an Al alloy.

Table 2. Recipes fro electrolytic polishing (see Fig. 22) and mechanical polishing (see Fig. 23).

Electrolytic polishing	Mechanical polishing
Electrolyte: 20 vol% perchloric acid (60%) and 80 vol% ethanol *Cell voltage*: 17 V *Time*: 20 s *Temperature*: -10°C	*Step 1*: 3-µm diamond on a satin woven acetate cloth (“DAC”, Struers) *Step 2*: 0.25-µm colloidal silica (pH 7) on a porous neoprene cloth (“Chem”, Struers)

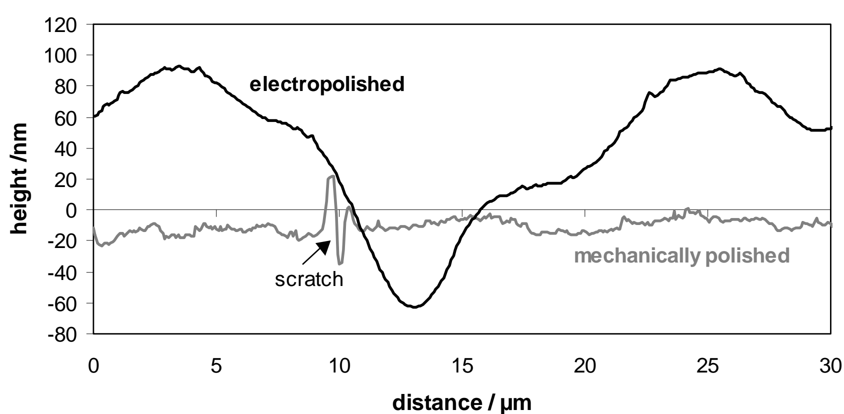

Fig. 24. Evaluation of the maximum tilt angles, about 1.5°, by profilometry of the electro-polished surface.

For example, the concentration of Cu was measured along a line on both prepared surfaces. The operation conditions are: 20 kV beam energy, 20 nA beam current, 10 s measuring time per point, LiF-crystal, Cu-Kα. For both methods a sensitivity of 5 rel% was determined, which corresponds to the statistical errors.

Thus, once electrolytic polishing procedures have been established, satisfactory results can be obtained rapidly, particularly for softer metals. The absence of scratches is also advantageous in acquiring high-quality electron microscopy images. In addition, artefacts resulting from mechanical damage do not occur in electro-polishing. This is particularly beneficial when using quantitative X-ray analysis in combination with EBSD.

Nevertheless, under some electro-polishing conditions, artefacts like dimples and pitting may be produced. Also, edge effects limit its application. In multiphase alloys, the rates of polishing of different phases depend on whether they are strongly cathodic or anodic with respect to the matrix. The result may be a non-planar surface. Additionally, electro-polished surfaces of certain materials may be passivated. In order to demonstrate this, mappings of O-Kα and Si-Kα were acquired in a region enriched with AlSi-phases. Electro-polishing causes a local oxidation of the AlSi-phases and a strong roughening of the surface (Fig. 25a), whereas the mechanical polishing delivers no artefacts (Fig. 25b). Furthermore, you have to be careful with handling electrolytes; many are poisonous, highly flammable or potentially explosive! Epoxy resin is one of the mounting materials, which can safely be used in contact with electrolytes containing $HClO_4$.

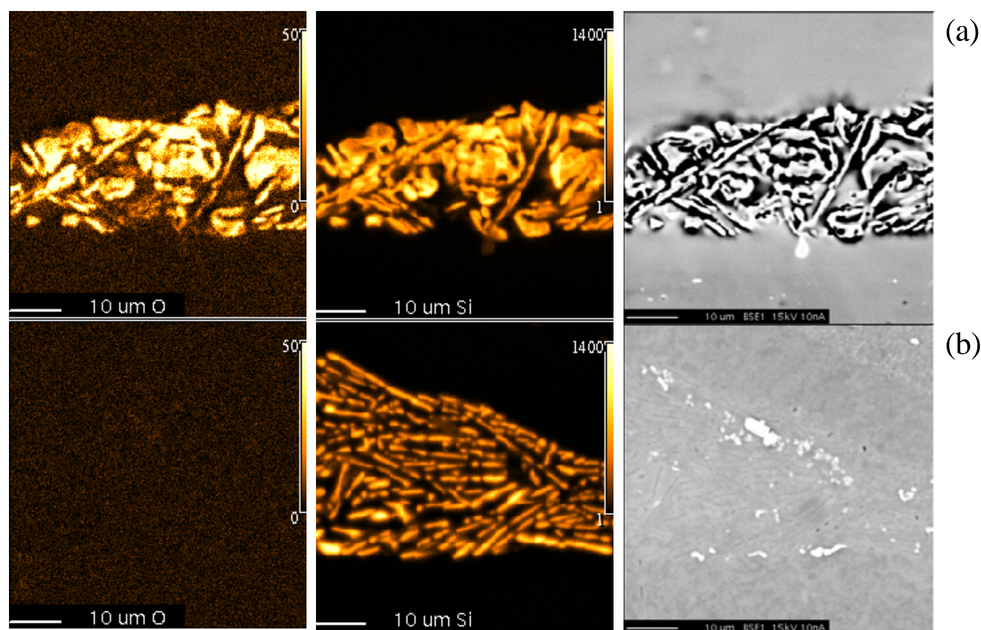

Fig. 25. (a) Roughening of the AlSi surface due to local oxidation under electro-polishing; (b) AlSi surface after mechanical polishing.

DIMPLE GRINDING

Conventional EPMA techniques, like analysis of a polished cross-section, result often in a depth resolution in the µm range owing to the interaction volume. The dimple grinding technique, together with small electron beam energies, makes it possible to increase the depth resolution to 100 - 150 nm [16, 17]. Therefore, it delivers an excellent method for the chemical characterisation of multilayered coatings on hard metal cutting tools. The technique is schematically presented in Fig. 26: a 20 mm ∅ ball of steel is rotating on the specimen's surface. With the help of 1 µm diamond suspension a dimple is produced. The optical microscopy image of a grinded dimple in a TiAlN-coating is shown in Fig. 27. Depending on the received angle of the bevel the thickness of the uncovered layers is broadened by a factor up to 100 (Fig. 28). Thus, a line scan can be performed along the bevel at low electron beam energy with an electron beam diameter of about 1 µm. For example, the characteristic X-ray intensities of Ti-Kα, Al-Kα, N-Kα and O-Kα were acquired during scanning the electron beam across the wedge (Figs. 29 and 30). The scan started at the top edge of the dimple and ended a few µm into WC/Co substrate. An electron beam energy of 7 kV, a beam current of 40 nA and bulk samples for calibration were used. By applying a matrix correction programme, the atomic fraction of each element versus distance *x* can be determined. Besides the rapid preparation another advantage is the determination of the depth scale. Provided that the radius *r* of the dimple is known and that the dimple is exactly a segment of a sphere, made with the known grinding ball radius *R*, the depth of the analysis can be calculated from the scanned distance x by using the equation:

$$d = \mathrm{sqrt}[R^2-(x-r)^2] - \mathrm{sqrt}[R^2-r^2]. \qquad (1)$$

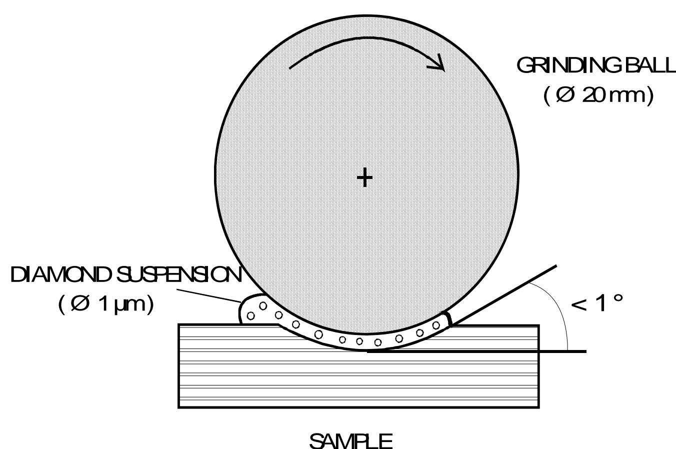

Fig. 26. Schematic representation of dimple grinding.

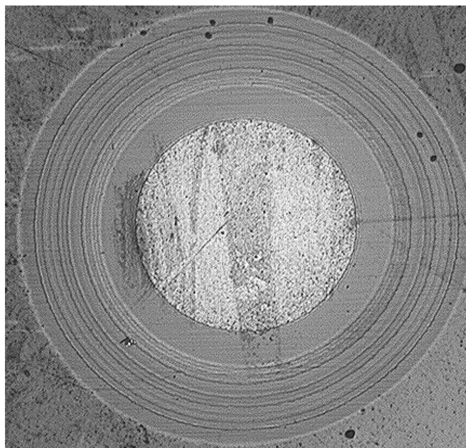

Fig. 27. Optical microscopy image of a grinded dimple in a TiAlN-coating.

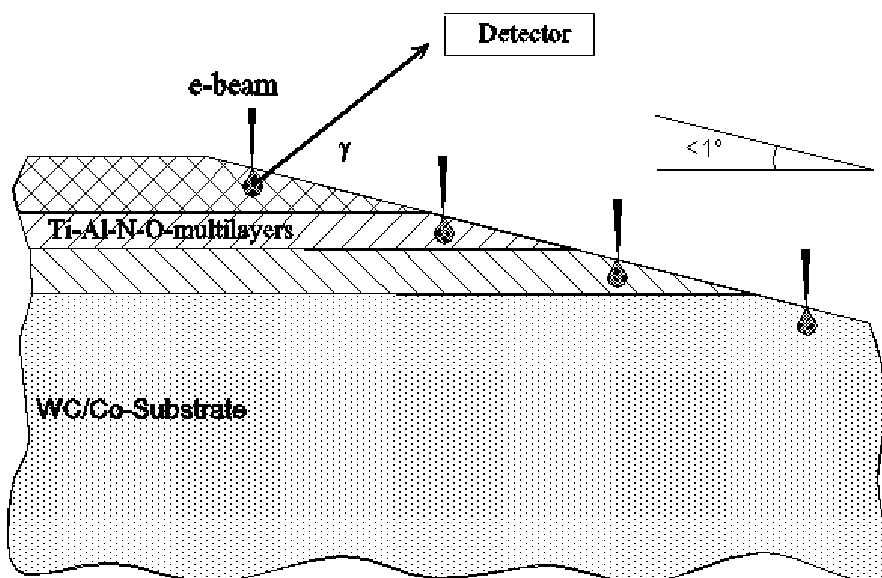

Fig. 28. Thickness of the uncovered layers.

Be aware that an inadequate preparation, which can lead to mechanical damage of the layers. The AFM-image (Fig. 31) shows broken interfaces in the dimple region. This artefact results in an erroneous depth profile, because the assumptions of Eq. (1) are not fulfilled. The artefact is visible in the very steep variation of atomic composition at the interface, for example, in a depth of 3,000 nm. This steep variation is inconsistent with the depth resolution of the method which can be estimated by the cumulative $\Phi(\rho z)$-function (absorption corrected), calculated by a Monte Carlo simulation or analytical models [5, 18].

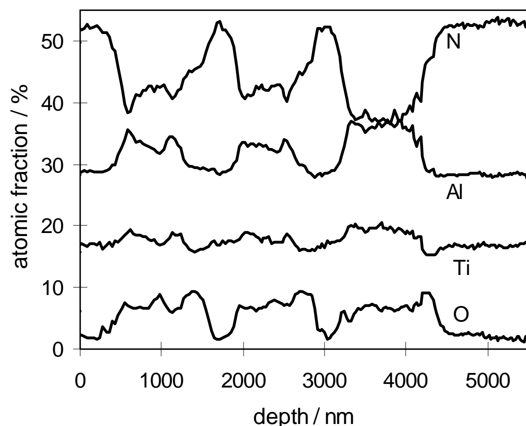

Fig. 29. Ti-Kα, Al-Kα, N-Kα and O-Kα X-ray intensities acquired during a scan across the wedge.

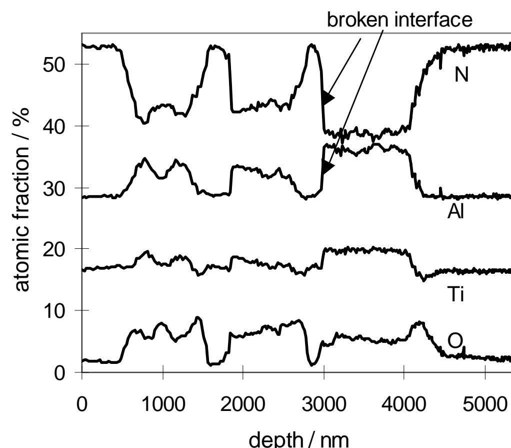

Fig. 30. Ti-Kα, Al-Kα, N-Kα and O-Kα X-ray intensities acquired during a scan across the wedge.

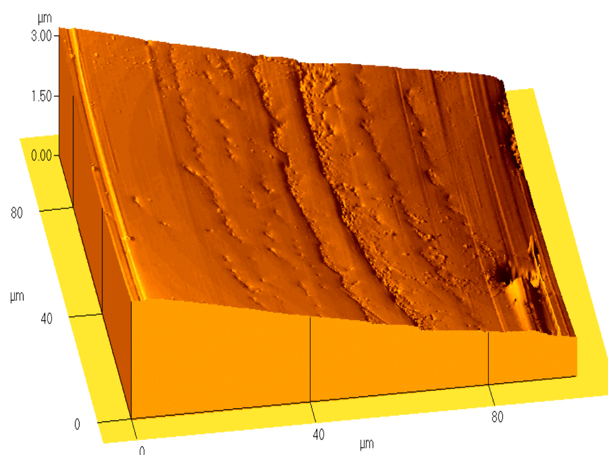

Fig. 31. AFM image showing the broken interfaces in the dimple region.

ION BEAM TECHNIQUE

Since the last 20 years, a new specimen preparation technique has been developed: the focused ion beam (FIB) technique [19]. The focused ion beam system uses a Ga ion beam. The advantage of Ga is the low melting point near room temperature and the very high percentage of Ga ions during emission. Thus, Ga is an ideal candidate for a liquid metal source for ion emission. This very small point source in combination with electrostatic lenses, delivers a focus of about 5 nm in diameter. Furthermore, excellent properties with respect to height control and depth of focus can be achieved. With these excellent properties of surface removal in mind, the ion beam is able to make a precise cut or cross-section. Qualitative X-ray

analysis can be acquired in an SEM by tilting the cross-section area towards the direction of the EDS detector. By combining SEM and FIB in a single so-called dual beam instrument, no sample transfers are required anymore eliminating any possible contamination. One advantage of the FIB-technique is that no edge rounding occurs at interfaces of phases with different hardness. Due to the low sputter angle, the sputter yield is nearly independent on the material's structure and composition. Another advantage is the ability to reveal small voids or other fragile features without the potential damage involved in mechanical preparation. FIB application in materials science has mainly been hampered by high costs and therefore limited availability of these instruments to the materials science community.

At our institute a special ion beam preparation technique for depth profiling was developed [20]. For example, a multilayered system Al / SiO_2 / GeSbTe // SiO_2 used in optical data storage was prepared by this technique (Fig. 32).

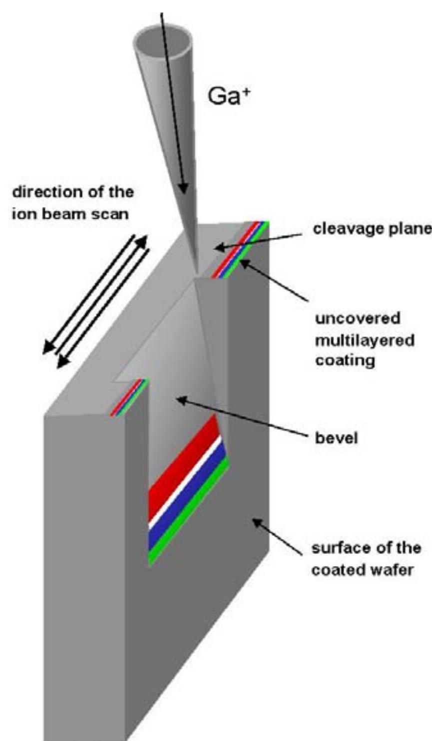

Fig. 32. Schematic drawing of a multilayered system Al / SiO_2 / GeSbTe // SiO_2, used in optical data storage, was prepared using FIB.

The coated wafer was cleaved and fixed on a holder in vertical direction. The Ga ion beam was focused on the cleavage plane with an angle of about 1° to the surface plane of the coating. A bevel was milled by scanning the beam over an area of about 0.5×20 μm^2. The uncovered layer system can be seen in the secondary electron image induced by the focused ion beam (Fig. 33). For contrast enhancement the multilayer system was coated by an Au-film before milling. The individual layers with sharp transitions can be distinguished very clearly.

The advantage of the FIB specimen preparation is the smooth bevel with defined geometry and a residual roughness on the nanometre scale. Furthermore, edge rounding is prevented, which is an ideal precondition for performing a line scan across the bevel. The measured characteristic X-ray intensities versus distance (Fig. 34a) can be compared with the ones calculated by means of a Monte Carlo simulation programme (Fig. 34b). As a result of this analysis, the layer system can be reconstructed as follows: Au (d = 42.5 nm) / Al (d = 133.4 nm) / SiO_2 (d = 41.6 nm) / $Ge_{2.6}Sb_{2.1}Te_{5.3}$ (d = 84.8 nm) // SiO_2. Further details can be found in [20].

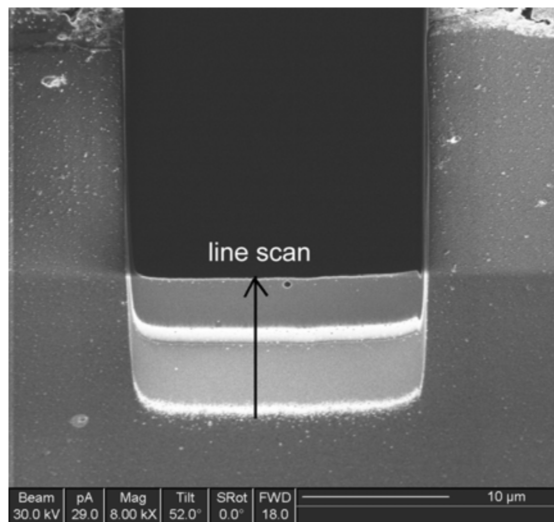

Fig. 33. Observation of the uncovered layer system, as seen in the secondary electron image induced by the focused ion beam.

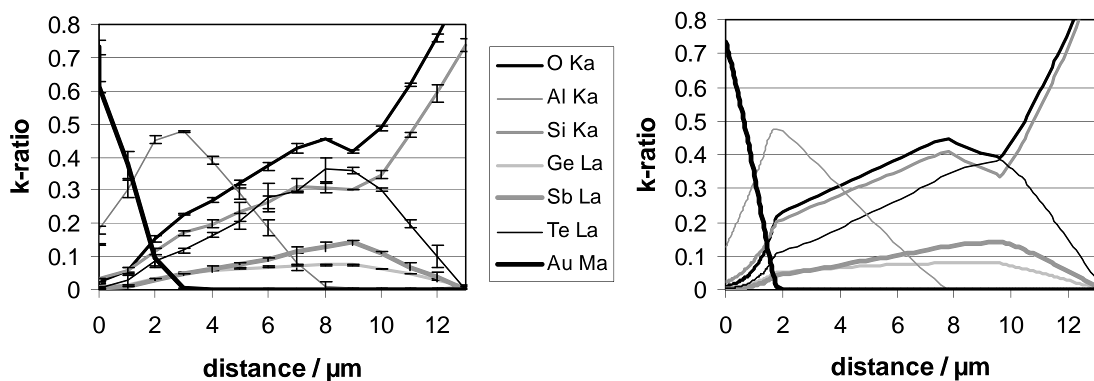

Fig. 34. (a) Measured characteristic X-ray intensities.
(b) Calculated characteristic X-ray intensities using a Monte Carlo simulation programme.

Let us demonstrate the excellent properties of the FIB ion beam technique with another example[21]. A fibre-matrix composite (Fig. 35) used for the development of materials in gas turbines.

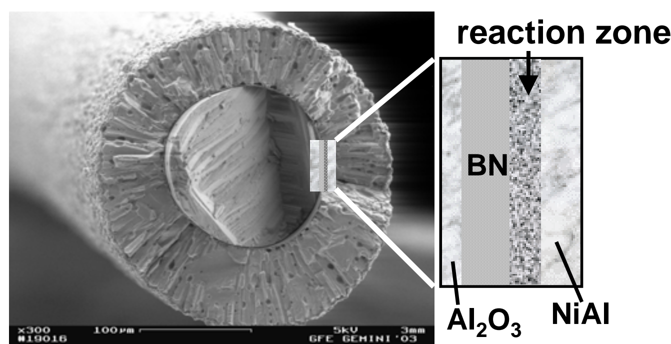

Fig. 35. Fibre-matrix composite used for the development of gas turbine materials.

To optimise the bonding strength, two layers consisting of BN and Hf are embedded between sapphire fibre and matrix. This fibre-matrix composite was annealed under an operating temperature of 1,350 °C. The aim was to characterise the reaction zone. This is a challenge regarding:

- the complex geometry;
- the different hardness of fibre and matrix;
- layers with thickness on the nanometre scale surrounded by a relatively thick layer.

In order to solve these problems the following preparation steps were applied. At first, the fibre could be pulled out of the matrix at the fracture surface of the BN-layer. Then the FIB-technique described in the previous example was applied (Fig. 36). The uncovered reaction zone is seen in the secondary electron image (Fig. 37). Voids are clearly visible. X-ray mappings (Fig. 38) were acquired for localising the reaction products, which were previously determined by XRD, and the diffusion zone. The EPMA user must be careful with the interpretation of the X-ray mappings due to the excitation volume and absorption of characteristic X-ray lines.

The main disadvantage of FIB techniques for materials science applications is the limited size of the specimen that can be produced using the FIB. A large FIB-produced cross-section would measure up to 100 - 200 µm in length and 10 - 20 µm in depth.

Thus, FIB in materials science is best used when a specific area of interest (grain boundary, corrosion pit, crack tips, films grown on surfaces, etc.) can be defined.

To prepare cross-sections with much larger areas, an Ar ion beam with a masking plate [22] can be used. The principle of such a cross-section polisher is illustrated in Fig. 39. Due to the masking plate the Ar ion beam is incident parallel to the cross-section. A smooth surface can be achieved by rocking the specimen around an axis perpendicular to the cross-section. It

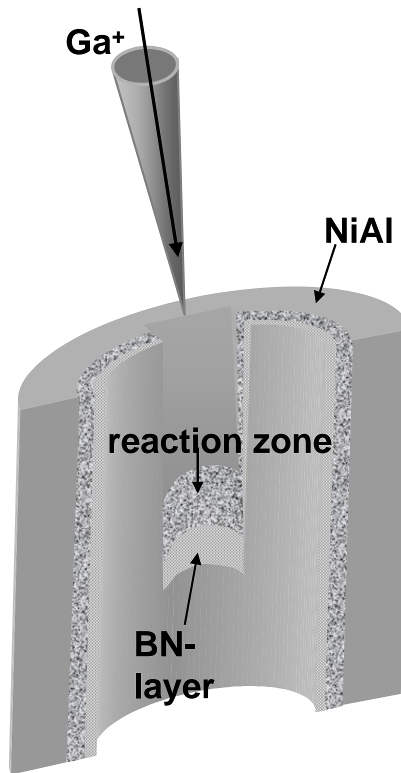

Fig. 36.

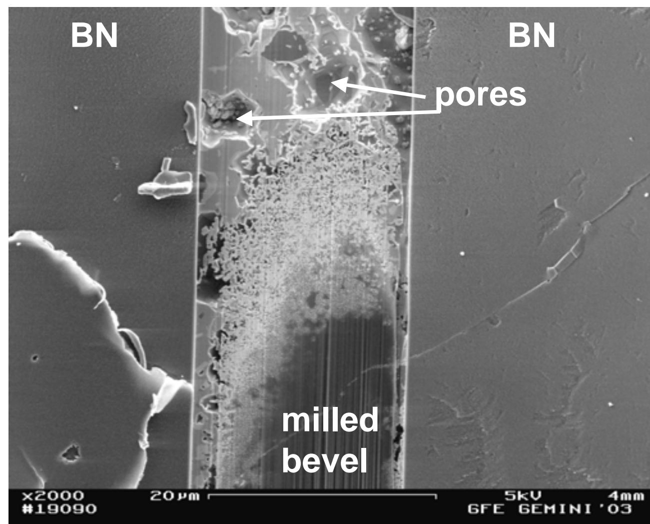

Fig. 37. Secondary electron image showing the uncovered reaction zone.

is reported [22] that the quality of the surface finish is similar to the one produced by the FIB-technique.

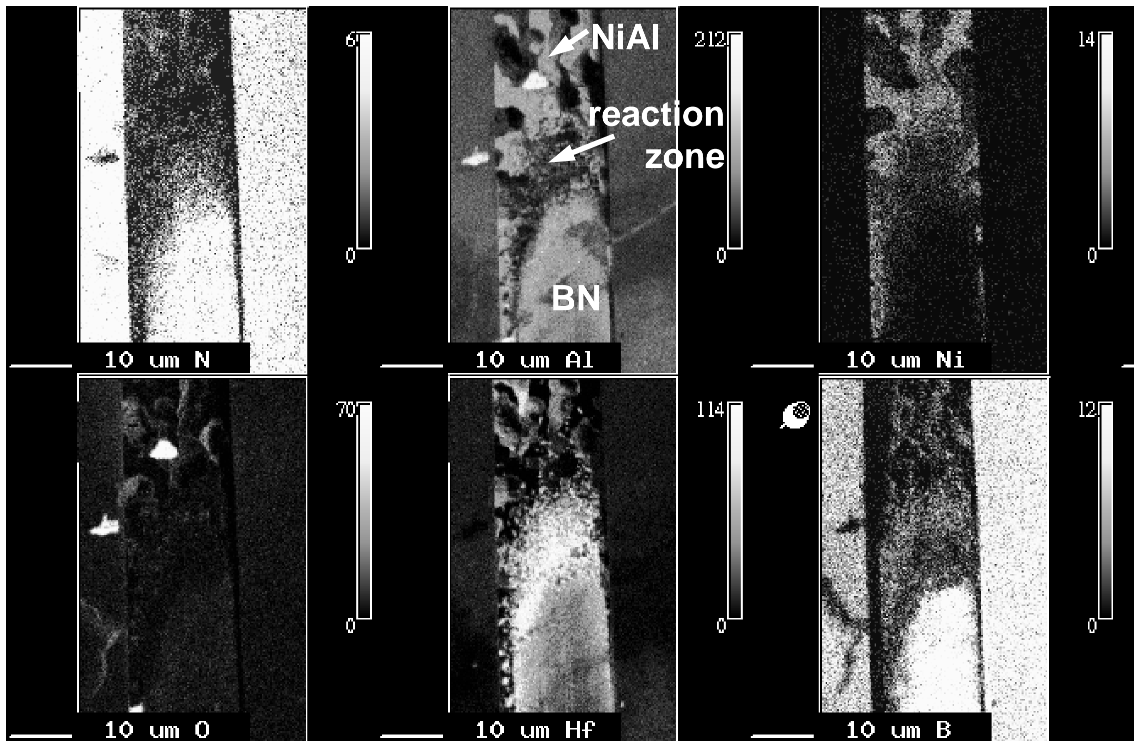

Fig. 38. X-ray mappings acquired for localising the reaction products.

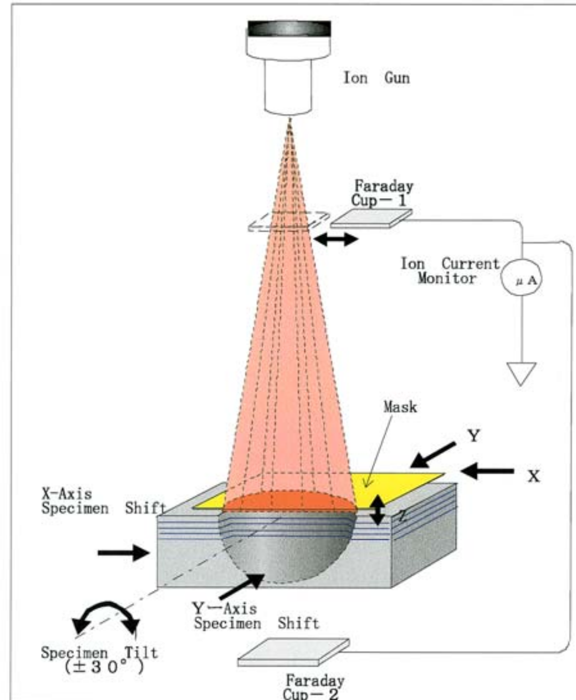

Fig. 39. Principle of cross-section polisher.

CONCLUSIONS AND SOME HELPFUL HINTS

Preparation techniques for light microscopy are also in common use for EPMA. The proper preparation steps for producing a sample are extremely important because the true microstructure or microchemistry of the sample may be obscured or altered by the use of an inappropriate technique. For light microscopy it was Sorby [23] in 1863, who succeeded in preparing the first true microstructure of steel. Sorby already knew that to reveal the true microstructure the surface of the metal required very careful treatment. But it took about one century until the importance of the preparation in revealing the true microstructure was studied by Samuels and Vilella [24]. They defined the true microstructure as being characterized by:

No deformation
No introduction of foreign elements
No scratches
No smearing
No pull-outs
No surface relief or edge rounding
No false microstructure
No thermal damage

This definition can also be applied to the preparation for EPMA with these additions:

No (further) charging effects
No contamination

The best preparation cannot fulfil all these conditions. A minimum amount of subsurface or surface damage will remain. Even if the light microscopic image reveals the true microstructure, the analysis in SEM or microprobe can lead to a misinterpretation, especially at low voltages, in light element analysis or trace analysis. Artefacts cannot be avoided, but the EPMA specialist should have a trained eye for recognizing them.

In qualitative microanalysis one must be careful to avoid the introduction of artefact X-ray peaks from the surrounding material, the polishing materials used or the specimen mounting material. A record of the materials used in the specimen preparation should be retained, in case a question arises subsequently on the source of possible contamination arises subsequently.

In quantitative analysis, the easiest way to detect a contaminated surface or fragmented near surface layer is to apply measurements at different electron beam energies (that means different information depths) and check the consistency. Preparation induced trapping sites for electrons in insulators can produce different charging effects, which can be revealed by determining the Duane-Hunt Limit (DHL) using an EDS detector. In the case of a conductive coating they can only be revealed by measuring X-ray intensities versus electron beam energy (see above). The influence of artefacts on quantitative X-ray analysis can be reduced, by using standards of known composition and preparing the standards in the same manner. To avoid alterations of surface composition during storage the analysis has to be performed as soon as possible. Sometimes it is necessary to prepare samples with 2 or 3 recipes to get reliable

results in EPMA. Depending on the aim of microanalysis, the influence of a specific artefact on the result is different. Since many laboratories have their own metallography, it is helpful for the EPMA specialist to discuss the preparation procedure with the metallographer before measurement. It is also helpful to write a preparation script in combination with a measurement protocol. This delivers experience for the future, saves time, costs and avoids misinterpretation of the microstructure or microchemistry.

Ion beam techniques are coming in and offer an excellent prepared surface for EPMA. Sputter effects within a depth of a few nm do not influence the quantitative analysis. Furthermore a tricky technique allows depth profiling in EPMA. Due to the high cost of the equipment, only a few labs enjoy possession of this technique.

ACKNOWLEDGEMENTS

The authors like to thank Michael Spähn for carrying out the EPMA measurements, Anke Aretz for the AFM studies, Werner Rehbach, Martina Schiffers and Melanie Keil for support in sample preparation, and finally all the co-workers and colleagues at GfE who contributed to this report.

REFERENCES

[1] G.W. Snedecor and W.G. Cochran (1980) *Statistical Methods, 7th ed.* Iowa State University Press, 243.

[2] J. Visman (1969) *A General Sampling Theory*. Mat. Res. Stand., 8.

[3] G.F. Vander Voort (1984) *Metallography: Principles and Practice*; McGraw-Hill.

[4] L. McCall and W.M. Mueller (1974) *Metallographic Specimen Preparation-Optical and Electron Microscopy*. Plenum Press, 41.

[5] N. Ammann and P. Karduck (1990) *Microbeam Analysis-1990* (J.R. Michael and P. Ingram, Eds.). San Francisco Press, San Francisco, 150.

[6] R. Gauvin and E. Lifshin (2000) *Mikrochim. Acta,* **132**, 201.

[7] *ASM Handbook, Vol. 9: Metallography and Microstructures*. ASM International, Metals Park, Ohio.

[8] B. Bousfield ( ) *Surface Preparation and Microscopy of Materials*. Wiley, New York.

[9] K. Geels (2000) *Prakt. Metallogr.*, **37**, 659.

[10] R. Gauvin (2004) *Microsc. Microanal.*, **10**, 669.

[11] G. Remond, C. Nockolds, M. Phillips and C. Roques-Carmes (2002) *J. Res. Natl. Inst. Stand. Technol.*, **107**, 639.

[11] N.J. Zaluzec, B.J. Kestel and D. Henriks (1997) *Microsc. Microanal.*, **3**, 983.

[12] B. Chapman (1980) *Glow Discharge Processing*. Wiley, New York.

[13] J. Goldstein et al. (2003) *Scanning Electron Microscopy and X-ray Microanalysis*. Springer, New York, 647.

[14] G.F. Bastin and H.J.M. Heijligers (2004) *Microsc. Microanal.*, **10**, 733.

[15] L.E. Samuels (1962) *Metallurgia*, **66**, 187.

[16] P. Willich and R. Bethke (1996) *Mikrochim. Acta*, Suppl. 13, 631.

[17] H. Blome (1996) IAESTE-Trainee Work, GFE, RWTH Aachen, Germany.

[18] J.-L. Pouchou and F. Pichoir (1984) - parts I and II *Rech. Aérosp.* 1984-5, 13 and 1984-5, 349.

[19] J. Orloff, M. Utlaut and L. Swanson (2003) *High Resolution Focused Ion Beams: FIB and its Application*. Kluwer Academic / Plenum Publishers, New York.

[20] S. Richter et. al. (2004) *Mikrochim. Acta*, **145**, 187.

[21] S. Richter et. al. (2006) *Mikrochim. Acta*, in press.

[22] H. Takahashi et al. (2005) in: "*Book of Abstracts of the 9th European Workshop on Modern Developments and Applications in Microbeam Analysis (EMAS2005)*", 22-26 May 2005, Florence, Italy.

[23] L.E. Samuels (1982) *Metallographic Polishing by Mechanical Methods*. American Society for Metals, Metals Park, Ohio.

[24] J.R. Vilella (1983) *Metallographic Technique for Steel*. American Society for Metals, Cleveland, Ohio, 1983.